Technical Note

Study of the Lateral Bearing Capacity and Optimization Reinforcement Scheme of an Open Caisson with Consideration of Soil Disturbance

An-Hui Wang [1], Yan-Fang Zhang [1], Fan Xia [1], Ru-Ping Luo [2,3,*] and Ning Wang [2,3]

[1] China Construction Industrial & Energy Engineering Group Co., Ltd., Nanjing 210023, China; wanganhui@cscec.com (A.-H.W.); zhangyanfang@cscec.com (Y.-F.Z.); xiafan@cscec.com (F.X.)

[2] School of Civil Engineering and Architecture, East China Jiaotong University, Nanchang 330013, China; wn1290@163.com

[3] Engineering Research & Development Centre for Underground Technology of Jiangxi Province, East China Jiaotong University, Nanchang 330013, China

* Correspondence: luo.ruping@outlook.com

Abstract: The bearing capacity of an open caisson under lateral loads is a key factor affecting the normal operation of an open caisson. It will inevitably have a disturbing effect on the surrounding soil layers during the sinking process of the caisson; that is, a disturbance ring will develop around the caisson. Based on the Jurong Yangtze River water supply project, the lateral bearing characteristics of the open caisson are analyzed by the numerical method with due consideration to soil disturbance, and the reinforcement scheme is optimized. The numerical results show that when the thickness of the disturbance ring is less than 0.5 m the disturbance ring has little effect on the lateral bearing capacity of the open caisson. An arc-shaped cement–soil reinforcement at the loading area can effectively improve the lateral bearing performance of the caisson. The optimized reinforcement thickness is 2 times that of the disturbance ring, and the reinforcement angle is approximately $60°$.

Keywords: open caisson; lateral bearing performance; disturbance ring; optimization reinforcement scheme; numerical simulation

1. Introduction

Pipe jacking technology is a non-excavation construction method developed after the shield method in underground pipeline engineering. It plays an increasingly important role in the construction of infrastructure such as electric power and municipal pipeline networks [1,2]. This technology usually needs to be carried out in a working well; the enclosure structure of the working well can be constructed of steel sheet piles, open caissons, diaphragm walls, and a composite retaining wall. The open caisson is widely used in underground pipeline engineering because of its high rigidity, good integrity, and convenient construction compared with other methods. During the construction of pipe jacking, it is necessary to set the counterforce frame in the inner wall of the caisson to provide horizontal jacking force; hence, the overall stability and deformation characteristic of the caisson under lateral load is one of the key factors for the normal operation of the pipe jacking [3]. If a large lateral shift or tilt occurs on the caisson shaft during the process of jacking, it will directly affect the accuracy of the pipe jacking, causing a significant risk to the structural safety of the caisson.

In order to investigate the deformation characteristics of caisson structures under lateral loads, a series of studies based on numerical simulations, theoretical analyses, and model tests have been conducted. For example, Coffman et al. [4] studied the displacement of the suction caisson when the horizontal load reaches the ultimate state. The results show that when the horizontal displacement of the caisson reaches 3% to 13% of the caisson diameter, the lateral bearing capacity reaches the limit state. Li et al. [5] used the scaled

model tests and finite-element numerical simulations to investigate the nonlinear tensile force–displacement patterns of the anchorage foundation in soft soil ground. Gerolymos and Gazetas [6–8] proposed a nonlinear design model based on the generalized Winkler model to calculate the displacement of the caisson under lateral static and cyclic loads, and the model was validated by model tests. Further, based on the three-dimensional finite element model, Sun et al. [9] investigated the deformation characteristic of the soil behind the reaction wall of an open caisson while considering the disturbance of the soil behind the reaction wall. The results showed that the reaction force has a significant effect on the deformation of the soil within the range of the reaction wall embedment depth.

In order to investigate the soil-structure interaction characteristics, an energy-based analysis and design framework for a soil-structure interaction system is presented by Yang et al. [10] in which energy dissipation in the soil and structural elastic plastic can be considered. Kechidi et al. [11] proposed a numerical tool based on the Monkey-tail fundamental lumped parameter model for the simulation of dynamic soil-structure interaction (SSI). Xue et al. [12] present experimental tests of four RC pile specimens backfilled with different damping material to assess their effect on the soil-structure hysteretic response. Mu et al. [13] studied the load–displacement curve of the caisson under different horizontal loads by a series of model tests, and the horizontal displacement of the soil in the passive area was investigated as well. In addition, Fu [14], Hu et al. [15], Faizi et al. [16], Zhao et al. [17], and Rachamadugu et al. [18] have investigated the deformation behaviour of an open caisson through model tests or numerical researches.

It should be noted that in the above studies, the horizontal load is applied at the top of the caisson to simulate the displacement characteristics of the caisson as a foundation structure. However, when the open caisson is used as the working well of a jacking pipe, the jacking load mainly acts at the bottom part of the caisson, and the displacement characteristics will be different from those found when the load acts on the top of the caisson. In addition, the influences of the caisson construction were not considered in the analysis of the lateral load response characteristics of the caisson in the current study. During the sinking of the caisson, there will inevitably be severe disturbance to the adjacent soil layers, and a disturbance ring will be developed along the circumference of the caisson. When an undrained sinking method is adopted, the effect of the soil disturbance will be more significant.

In view of this, based on the pipe jacking project of Jurong Water Plant, a series of numerical simulations via Plaxis 3D are conducted to analyze the influences of the disturbance ring on the lateral bearing characteristics of the caisson. The objective of this paper is to evaluate the lateral bearing capacity of an ultra-deep open caisson under lateral pipe jacking force and to put forward an optimization reinforcement scheme to improve the horizontal stiffness and reduce the lateral displacement of the open caisson. The high-pressure rotary jetting is used as the caisson reinforcement construction scheme. The lateral load–displacement patterns of the caisson under different reinforcement areas are analyzed, and an optimized design plan of caisson reinforcement is proposed. The originality of this paper lies in the consideration of the soil disturbance ring around the perimeter of the caisson, which can reveal the bearing capacity characteristics of the caisson foundation more accurately. The findings of this paper aim to provide a reference for similar projects.

2. Project Overview

Jurong Yangtze River water intake project is located in Xiashu Town, Jurong City, Jiangsu Province, which includes a water source located on the north side of the main channel of Yangtze River, a water intake artesian pipe across the Yangtze River, and a water intake pumping station, as shown in Figure 1. Taking water from the Yangtze River channel and pumping it to the water plant for processing meets the water demand of Jurong city residents. Two open caissons used as the starting wells for the Yangtze River water intake pipeline are installed within 300 m of the Yangtze River dam. The caisson depth is 46.5 m and the outer diameter is 16 m (as shown in Figure 2). The length of the pipeline from the

water source to the pipe jacking wells is approximately 1.4 km, of which the length of the underwater pipeline is 1.3 km.

Figure 1. The location of the Jurong Yangtze River water intake project.
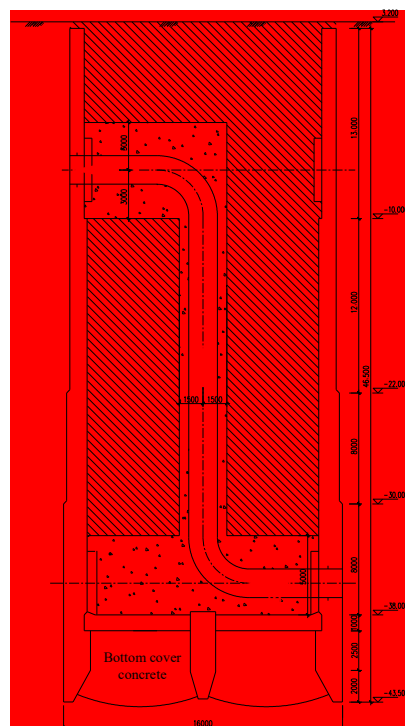

Figure 2. Schematic diagram of an open caisson.

The open caisson is located at a typical river flood plain and river terrace, with soft silty clay in the upper part and a highly permeable sand layer in the lower part. Due to the downward incision of the Yangtze River, the sand layer is connected with the surface water system and is rich in water content. According to the results of field drilling and in situ testing, except the filling in of the shallow part, the soil layer within the exploration depth of 70 m in this survey is widely distributed by Holocene estuarine facies silty clay with gray-yellow soft plastic or slightly dense silt with silty clay, coastal neritic gray flow plastic silty soil, gray silt of slight to medium density, and silty sand (partially mixed with silty clay). The silt, silty sand, and silty clay often interact multiple times. In the deep part of the ground, the soil layer is distributed by Pleistocene marina, neritic or estuarine delta

facies gray soft plastic silty clay, and gray-greenish gray with slight to medium density silt or silty sand. A typical stratigraphic profile is shown in Figure 3.
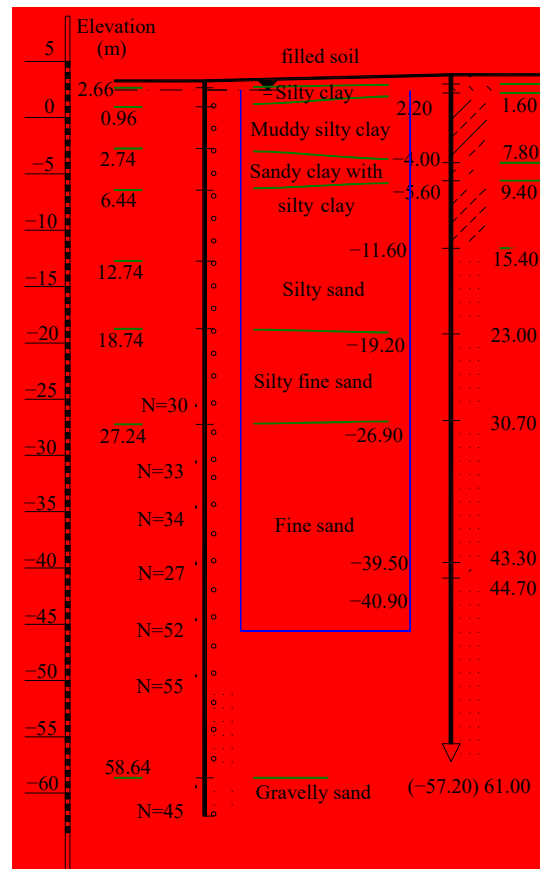

Figure 3. Schematic diagram of the site stratigraphy distribution.

The cone penetration curves of the stratum are shown in Figure 4, from which can be seen that the stratum exhibits significant stratification characteristics. The stratum within 10 m is mainly silty soil except for the thin hard crust layer at the ground surface. The average cone tip resistance q_c and side friction resistance f_s are approximately 0.5 MPa and 10 kPa, respectively. The bearing capacity of the soil layer increases with depth, and the average cone tip resistance q_c and side friction resistance f_s in the depth range of 10 m to 22 m are approximately 5.5 MPa and 55 kPa. With the further increase in depth, the stratum is mainly composed of compact sand layers, and the cone tip resistance and side friction resistance increase significantly. In general, due to the weak bearing capacity and lateral soil resistance in the shallow part (within the depth of 22 m), it is necessary to pay more attention to the lateral displacement and inclination of the caisson under lateral loads.
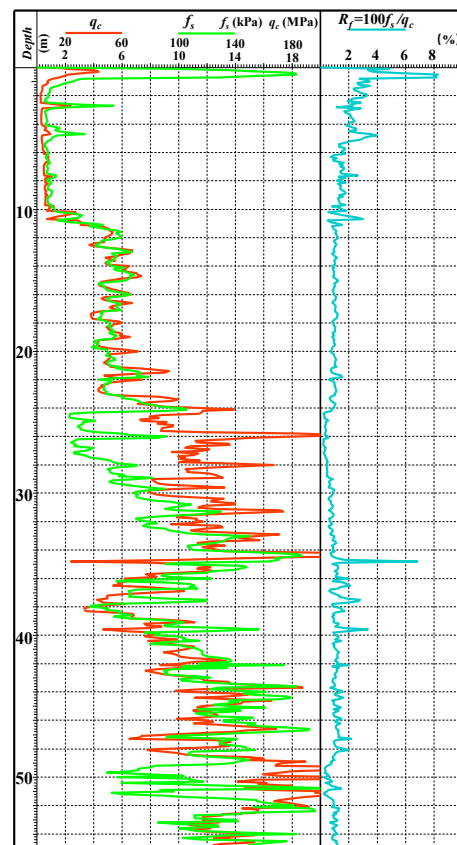
**Figure 4.** The cone penetration curves of the site.

3. Numerical Model

In this project, an ultra-deep caisson is used as the receiving well for water intake pipe jacking. The length of the pipeline from the water source to the caisson is about 1.4 km, and the diameter of the water intake pipe is 1.8 m. In order to jack the water pipe into the water source, it needs to exert a reaction force on the side wall of the caisson. Due to the large diameter and long distance of the water intake pipeline, and the fact that the stratum at the depth of the pipeline is mainly a sand layer, the reaction force acting on the sidewall of the caisson is very large. In order to investigate the overall stability of the caisson, a series of numerical simulations via Plaxis 3D are conducted to analyze the load–displacement characteristics of the caisson under the jacking force.

Figure 5 is a schematic diagram of the numerical analysis model for the bearing and deformation characteristics of the caisson under lateral jacking force. In the numerical model, fixed constraints are adopted at the bottom of the model and normal constraints are adopted at the sides. A horizontal force is applied at the inner wall of the caisson, within the same depth with the water intake pipeline. In order to be more consistent with the actual situation, the soil disturbance ring caused by the caisson sinking is considered in the numerical model. A disturbance ring with a different thickness is set around the caisson wall in the numerical model, and the mechanical parameters are reduced for the disturbance layer. In addition, the soil outside the shaft wall used for the jacking force is usually reinforced in the actual engineering to ensure that the caisson will not undergo excessive lateral displacement and inclination (as shown in Figure 5). By comparing the deformation characteristics of the caisson under fan-shaped reinforcement (Figure 5b) with those without reinforcement, the effect of soil reinforcement outside the shaft wall is evaluated and the optimized reinforcement range is proposed.
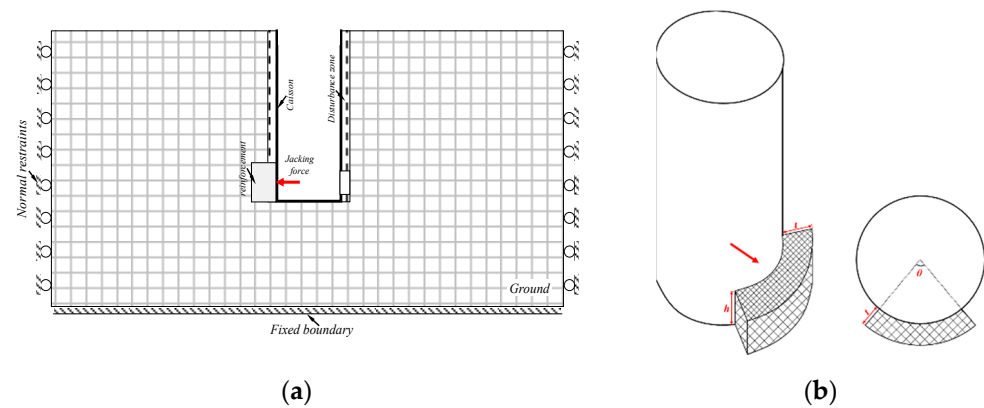
Figure 5. Schematic diagram of the numerical model: (**a**) Model profile view; (**b**) Schematic diagram of soil reinforcement.

Figure 6 is the numerical analysis model for the open caisson under lateral loads. The size of the numerical model is 200 m × 100 m × 80 m (length × width × depth). The caisson depth is 46.5 m, and the caisson diameter is 16 m, which can ensure that the boundary conditions have no effect on the calculation results [19]. In the numerical model, the caisson wall is simulated by the plate structure element with equal thickness to improve the calculation efficiency (the average wall thickness of the caisson structure at different heights in the original design). It should be noted that, due to the small length–diameter ratio of the open caisson, the overall deformation characteristic of the caisson appears as rigid rotation. Simplifying the caisson wall with unequal thickness to the wall with equal thickness will not affect the overall deformation characteristics of the structure. In addition, in the numerical model of this paper, the bottom cover concrete of the open caisson is also simplified as a plate structure element, and the plate thickness is the actual thickness of the bottom cover concrete (as shown in Figure 2).
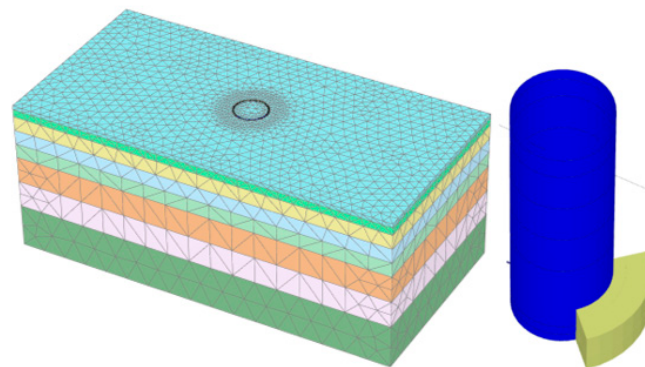
Figure 6. Diagram of finite element numerical model.

The interactions between the caisson foundation and the surrounding soil are modeled by the interface elements with Mohr–Coulomb failure criterion in Plaxis. These interfaces have properties of friction angle, cohesion, dilation angle, tensile strength, Young's modulus, and Poisson's ratio. The values of interface properties in Plaxis can be set by a reduction factor ($R_i \leq 1.0$) applied to the soil material when defining soil property values (the default value is $R_i = 1.0$, i.e., a fully-bonded interface). Hence, the interface property values are directly related to the mechanical properties of the soil around the interface. In this paper, a reduction factor $R_i = 0.7$ is adopted for the caisson-soil interface, which is similar to that for the pile foundation.

The constitutive model of ground soil, disturbance soil, and cement–soil reinforcement area adopts the Mohr-Coulomb criterion. The Mohr-Coulomb model has the advantages of having fewer input parameters and being easy to obtain in laboratory testing, and it

has been widely used in deep foundation analysis [20,21]. The input parameters of the ground soil in this paper are determined from geological reports and laboratory testing results. As discussed by Oteuil et al. [22], the elasticity modulus of ground soil (*E*) is a crucial parameter in the analyses of bearing capacity and deformation. This parameter is correlated from CPT results using a local empirical model [23]. Since the disturbance ring is mainly affected by the sinking of the caisson and the infiltration of friction-reducing mud, its material parameters are less affected by the corresponding soil layer. To simplify the calculation and analysis, the soil in the disturbance ring is assumed to be uniformly distributed along the depth direction. It should be noted that the bearing capacity of the caisson foundation is very sensitive to the soil parameters. In general, the bearing capacity of the caisson foundation decreases with the weakening of the soil mechanical parameters. Due to space limitations, this paper does not analyze the specific influence of soil parameter uncertainty on the bearing performance of the caisson foundation, and relevant discussion can be referred to Charlton & Rouainia [24] and Oteuil et al. [22]. Table 1 shows the parameters for soil or structures adopted in the numerical model.

Table 1. Material parameters in the numerical model.

Material	Thickness (m)	Cohesion c (kPa)	Friction Angle φ (°)	Unit Weight γ (kN/m^3)	Elastic Modulus E (MPa)
Silty clay	2.2	15.5	13.6	18.0	15.8
Muddy silty clay	4.0	14.9	13.8	17.7	14.2
Sandy silt 1	7.6	6.8	31.1	19.2	37.2
Sandy silt 2	7.6	6.2	32.6	19.2	39.9
Silty sand	7.7	6	29.4	19.3	38.6
Fine sand 1	14.0	3.7	34.1	20.3	40.7
Fine sand 2	14.1	6.3	32.7	19	41.8
Medium fine sand	25.0	3	35.3	19.8	44.7
Disturbed soil	-	15.0	5.0	18.0	5.0
Cement mixed soil	-	500	30.0	20.0	100.0
Concrete	-	-	-	25	40×10^3

Table 2 shows the analysis cases of the numerical simulations in this paper. The numerical analysis cases include two main parts: the influence of the thickness of the disturbance ring, and the influence analysis of the cement–soil reinforcement range. As shown in Figure 5b, the fan-shaped reinforcement area includes the reinforcement thickness t and the reinforcement angle θ. A total of 12 groups of working conditions are analyzed in this paper.

Table 2. Numerical simulation analysis conditions.

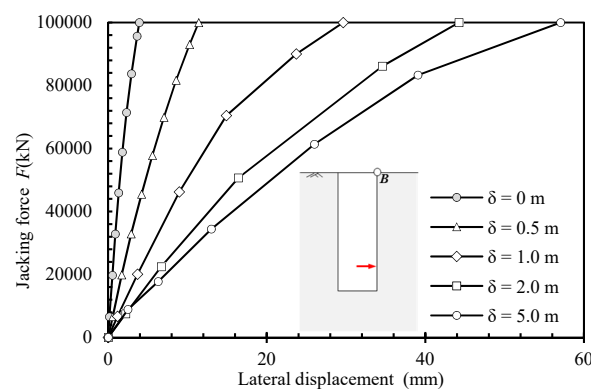| Thickness of Disturbance Ring δ (m)	Thickness of Reinforcement t (m)	Angle of Fan-Shaped Reinforcement θ (°)
0		
0.5		
1	-	-
2		
5		
	2	
	4	
	6	90
2	8	
		60
	4	120
		180

4. Analysis of Numerical Results

4.1. The Lateral Deformation Characteristics of a Caisson without Reinforcement

The load–lateral displacement curves at the loading point and ground surface under different thicknesses of the disturbance ring are shown in Figures 7 and 8. It can be seen intuitively from the figures that as the thickness of the disturbance ring increases, the horizontal stiffness of the caisson is attenuated, resulting in a larger horizontal displacement under the same horizontal load. Compared with the horizontal displacement of the caisson at the surface, the horizontal displacement at the loading point is more affected by the thickness of the disturbance ring. When the thickness of the disturbance ring is 5 m, the maximum horizontal displacement is close to 200 mm. It is worth pointing out that when the thickness of the disturbance ring is 0 m and 0.5 m, respectively, the load–horizontal displacement curve at the loading point has little difference. The possible reason is that when the thickness of the disturbance ring is within 0~0.5 m, the ratio of the disturbance ring thickness δ to the caisson diameter D is relatively small, and the horizontal resistance of the caisson is mainly provided by the surrounding undisturbed soil.
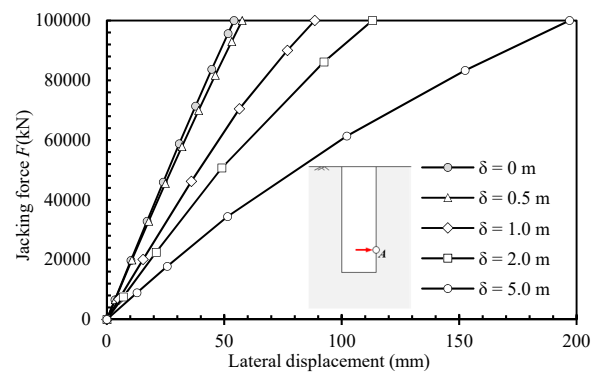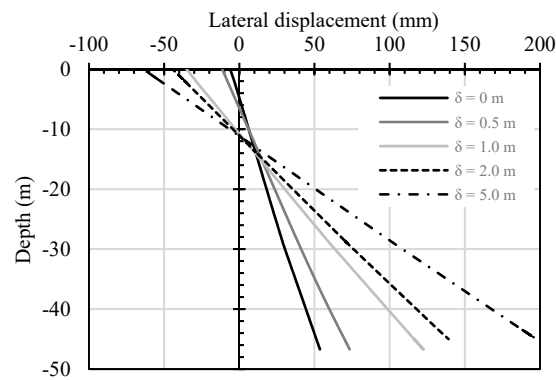

Figure 7. Load–lateral displacement curves at loading points under different thicknesses of the disturbance ring.
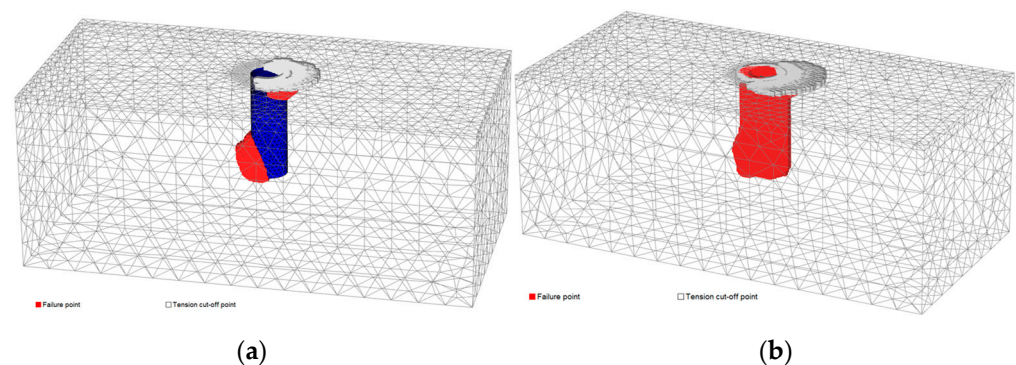

Figure 8. Load–lateral displacement curves at the ground surface with different thicknesses of the disturbance ring.

Figure 9 shows the lateral displacement distribution curves along the caisson depth under different disturbance ring thicknesses when the lateral jacking force reaches 1×10^5 kN. It can be seen that because the caisson length-to-diameter ratio is $L/D = 3.2$, which is similar to the rigid pile under a lateral load, the lateral displacement curve of the caisson along its depth is distributed linearly. In general, the position of the rotating center decreases with the increase in the thickness of the disturbance ring. When the thickness of the disturbance ring δ exceeds 1 m, the rotating center basically stabilizes at about 10 m below the surface, which is about 0.22 times the embedment depth of the caisson.

Figure 9. Variation curve of horizontal displacement along the caisson depth with different thicknesses of the disturbance ring.

Figure 10 shows the distribution of the plastic zone of the soil under different disturbance ring thicknesses, from which it can be intuitively seen that when the thickness of the disturbance ring is 0, the caisson undergoes rotational deformation, producing plastic failure areas in the opposite direction of the bottom loading point and in the shallow area. In addition, tensile failure occurs at the ground surface as well. In comparison, when the thickness of the disturbance ring is 2 m, the overall horizontal displacement of the caisson under a lateral jacking load is more pronounced as the disturbance ring soil undergoes complete plastic failure due to the poor mechanical properties of the soil in the disturbance ring.


Figure 10. Distribution of the soil plastic zone under different thicknesses of the disturbance ring: (**a**) $\delta = 0$ m; (**b**) $\delta = 2$ m.

4.2. Lateral Deformation Characteristics of a Caisson with Reinforcement
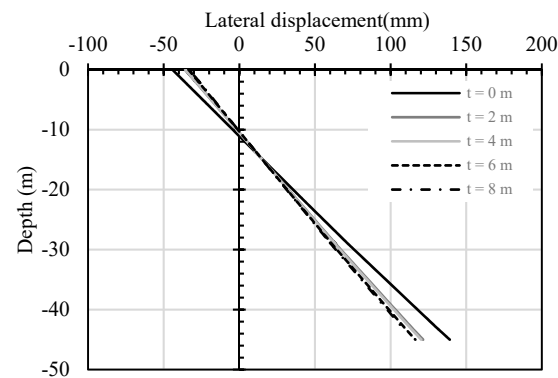
4.2.1. Influence of Reinforcement Thickness

In order to reduce effectively the influence of the disturbance ring on the lateral bearing performance of the caisson, the outer soil of the caisson at the loading point is reinforced. As shown in Figure 5b, the reinforcement area is fan-shaped with a reinforcement height of $h = 4$ m. Figure 11 shows the load–lateral displacement distribution curve at the loading point of the caisson for different reinforcement thicknesses t when the thickness of the disturbance ring δ is 2 m and the angle of the fan-shaped reinforcement θ is 90°. It can be seen from the figure that reinforcement of the soil at the loading point can effectively increase the horizontal stiffness of the caisson and reduce the lateral displacement. However, when the reinforcement thickness t exceeds 4 m (2 times the thickness of the disturbance ring), increasing the thickness of the reinforcement zone will not further improve the lateral bearing capacity of the caisson. Therefore, it is recommended that the thickness of the reinforcement area not exceed 2 times the thickness of the disturbance ring in practical engineering, in order to minimize the cost of the project and the difficulty of construction.
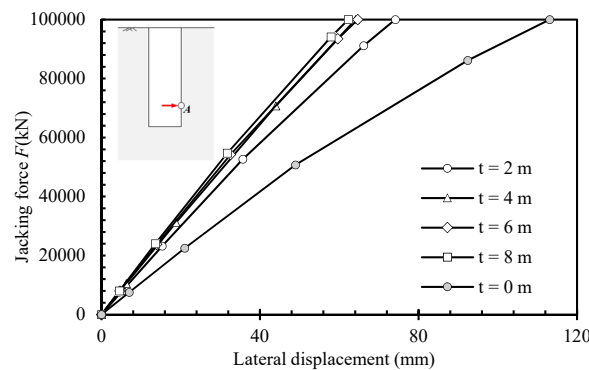
Figure 11. The load–lateral displacement curve of a caisson with different reinforcement thicknesses.

Figure 12 shows the variation curve of the lateral displacement of a caisson along the depth for different reinforcement thicknesses, which is consistent with the deformation characteristics of a caisson without reinforcement. In addition, when the reinforcement thickness exceeds 2 m, the lateral displacement of the caisson cannot be further reduced by continuing to increase the thickness of the reinforcement.

Figure 12. The variation curve of lateral displacement along the depth of a caisson with different reinforcement thicknesses.

4.2.2. The Influence of the Reinforcement Angle

In addition to the reinforcement thickness, the effect of the reinforcement angle on the lateral performance of the caisson is further analyzed in this section. In the numerical analysis, the height of the caisson reinforcement $h = 4$ m, the thickness $t = 4$ m, and the thickness of the disturbance ring $\delta = 2$ m. The load–lateral displacement distribution curves at the loading points of the caisson for different reinforcement angles are shown in Figure 13. It can be seen from the figure that the horizontal stiffness of the caisson increased with the gradual increase in the reinforcement angle. However, when the reinforcement angle is greater than 60°, continuing to increase the reinforcement angle has little effect on improving the horizontal stiffness and reducing the horizontal displacement of the open caisson, and the optimum reinforcement angle is approximately 60°.

Similarly, the variation in the horizontal displacement of the caisson with depth can be analyzed for different reinforcement angles, as shown in Figure 14. It can be seen from the figure that the caisson presents rigid rotational deformation at different reinforcement angles, and the optimum reinforcement angle is approximately 60°.

Based on the analysis above, it can be seen that the caisson presents a rigid rotating deformation under lateral jacking force acting at the bottom of the caisson. The rotating center is about 0.2 times the caisson embedment depth, which is quite different with the rotation depth (about 0.7~0.8 times of the caisson embedment depth) when the lateral load is acting at the pile top. In order to improve the lateral stiffness of the caisson effectively, high-pressure rotary jetting can be used to reinforce the soil outside the caisson. A preferred

reinforcement thickness is roughly twice the thickness of the disturbance ring, and the reinforcement angle is about 60°.
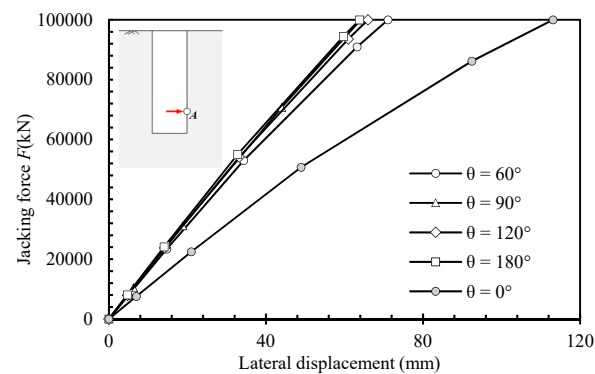
Figure 13. The load–lateral displacement curve of a caisson with different reinforcement angles.
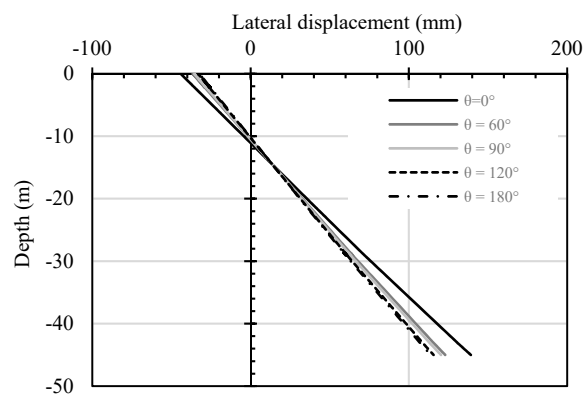
Figure 14. The distribution curve of lateral displacement along the depth of a caisson with different reinforcement angles.

5. Conclusions

Based on the Jurong Yangtze River water intake project, the three-dimensional numerical finite element Plaxis was adopted to analyze the lateral load bearing characteristics of an open caisson. The influence of the disturbance ring on the deformation characteristics of the caisson was investigated. Further, the reinforcement effects under different reinforcement schemes were analyzed. The main conclusions are as follows:

1. With the increase in the thickness of the disturbance ring, the horizontal stiffness of the caisson will gradually weaken. However, when the thickness of the disturbance ring is within 0.5 m, the effect of the disturbance ring on the load–horizontal displacement curve of the caisson will be reduced.

2. Under the action of horizontal load, the horizontal displacement of the caisson structure will manifest as rigid rotational deformation along the depth, and the position of the rotation center decreases with the increase in the thickness of the disturbance ring. When the thickness of the disturbance ring exceeds 1 m, the rotation center is basically stable at the depth of 0.2 times the caisson embedment depth.

3. The horizontal stiffness of the caisson increases with the thickness of the reinforcement. However, when the thickness of the reinforcement is more than twice the thickness of the disturbance ring, the lateral bearing capacity of the caisson will not be further improved by increasing the thickness of the reinforcement.

4. With the increase in the reinforcement angle, the horizontal stiffness of the caisson is increased gradually. When the reinforcement angle is greater than 60°, increasing the reinforcement angle has little effect on reducing the caisson horizontal displacement.

References

1. Thomson, J. *Pipejacking and Microtunnelling*; Springer: Boston, MA, USA, 2013.
2. Ma, B.; Zhou, W. China's Municipal Pipelines: Today and Tomorrow. In Proceedings of the Pipelines 2013: Pipelines and Trenchless Construction and Renewals—A Global Perspective, Fort Worth, TX, USA, 23–26 June 2013; pp. 10–18.
3. Sun, Y.; Shen, S.; Xu, Z.; Xia, X. Prediction of lateral displacement of soil behind the reaction wall caused by pipe jacking operation. *Tunn. Undergr. Space Technol.* **2014**, *40*, 210–217. [CrossRef]
4. Coffman, R.A.; El-Sherbiny, R.M.; Rauch, A.F.; Olson, R.E. Measured horizontal capacity of suction caissons. In Proceedings of the Offshore Technology Conference, Houston, TX, USA, 3–6 May 2004.
5. Li, J.; Zhang, Z.; Huang, H.; Li, Y.S. Research on Similarity Model Test of Anchorage of Qing-Feng Suspension Bridge in Ningbo. *J. Tongji Univ.* **2005**, *33*, 1011–1016.
6. Gerolymos, N.; Gazetas, G. Winkler model for lateral response of rigid caisson foundations in linear soil. *J. Soil Dyn. Earthq. Eng.* **2006**, *26*, 347–361. [CrossRef]
7. Gerolymos, N.; Gazetas, G. Static and dynamic response of massive caisson foundations with soil and interface nonlinearities—Validation and results. *J. Soil Dyn. Earthq. Eng.* **2006**, *26*, 377–394. [CrossRef]
8. Gerolymos, N.; Gazetas, G. Development of Winkler model for static and dynamic response of caisson foundations with soil and interface nonlinearities. *J. Soil Dyn. Earthq. Eng.* **2006**, *26*, 363–376. [CrossRef]
9. Sun, Y.; Su, J.; Xia, X.; Xu, Z. Numerical analysis of soil deformation behind the reaction wall of an open caisson induced by horizontal parallel pipe-jacking construction. *Can. Geotech. J.* **2015**, *52*, 2008–2016. [CrossRef]
10. Yang, H.; Wang, H.; Jeremić, B. An energy-based analysis framework for soil structure interaction systems. *Comput. Struct.* **2022**, *265*, 106758. [CrossRef]
11. Kechidi, S.; Colaço, A.; Costa, P.A.; Castro, J.M.; Marques, M. Modelling of soil-structure interaction in OpenSees: A practical approach for performance-based seismic design. *Structures* **2021**, *30*, 75–88. [CrossRef]
12. Xue, J.; Aloisio, A.; Lin, Y.; Fragiacomno, M.; Briseghella, B. Optimum design of piles with pre-hole filled with high-damping material: Experimental tests and analytical modeling. *Soil Dyn. Earthq. Eng.* **2021**, *151*, 106995. [CrossRef]
13. Mu, B.; Li, X.; Gong, W.; Jia, P.; Zheng, W. Model tests on deformation characteristics of caissons under long-term horizontal load. *Chin. J. Geotech. Eng.* **2017**, *39*, 1388–1397. (In Chinese)
14. Fu, S. *Study on the Lateral Bearing Properties of Root Stalk Caisson*; Southeast University: Nanjing, China, 2008. (In Chinese)
15. Hu, F.; Gong, W.; Yin, Y.; Tong, X.; Shan, J. Analysis of lateral bearing capacity of rigid root-foundation. *J. Mech. Eng.* **2010**, *32*, 67–71. (In Chinese)
16. Faizi, K.; Faramarzi, A.; Dirar, S.; Chapman, D. Development of an analytical model for predicting the lateral bearing capacity of caisson foundations in cohesionless soils. *J. Ocean. Eng.* **2020**, *218*, 108112. [CrossRef]
17. Zhao, X.; Zhan, W.; Yan, X.; Wang, J.; Yang, Z.; Gong, X. Experimental study and simulation on deformation characteristics of caissons in sand under horizontal loads. *Chin. J. Geotech. Eng.* **2021**, *43*, 80–83.
18. Rachamadugu, R.; Vikash, G. Lateral Response of Hollow Circular Caisson Embedded in Nonlinear Soils. *Int. J. Geomech.* **2022**, *22*, 04021275. [CrossRef]
19. Jin, Z.; Yin, Z.Y.; Kotronis, P.; Li, Z. Advanced numerical modelling of caisson foundations in sand to investigate the failure envelope in the HMV space. *J. Ocean. Eng.* **2019**, *190*, 106394. [CrossRef]

20.   Pei, T.; Qiu, T. A Numerical Investigation of Laterally Loaded Steel Fin Pile Foundation in Sand. *Int. J. Geomech.* **2022**, *22*, 04022102. [CrossRef]

21.   Sheil, B.; Templeman, J. Bearing capacity of open caissons embedded in sand. *Géotechnique.* **2022**, *72*, 1–11. [CrossRef]

22.   Oteuil, A.; Oralbek, A.; Mukhamet, T.; Moon, S.-W.; Kim, J.; Tokbolat, S.; Satyanaga, A. Robust Analysis and Design of Bored Pile Considering Uncertain Parameters. *J. Indian Geotech. J.* **2022**, *52*, 720–734. [CrossRef]

23.   Zhang, H. *Research on the Evaluation of Engineering Characteristic of the Loose Sediment in the North of Yangtze River Estuary*; Southeast University: Nanjing, China, 2005. (In Chinese)

24.   Charlton, T.S.; Rouainia, M. Probabilistic capacity analysis of suction caissons in spatially variable clay. *J. Comput. Geotech.* **2016**, *80*, 226–236. [CrossRef]